Fatigue life prediction of pedicle screw for spinal surgery

Š. Major
The Institute of Theoretical and Applied Mechanics, Academy of Science, Prosecká 809/76, 19000 Praha 9, Czech Republic
major@itam.cas.cz

V. Kocour
The Institute of Theoretical and Applied Mechanics, Academy of Science, Prosecká 809/76, 19000 Praha 9, Czech Republic
kocour@itam.cas.cz

P.Cyrus
Department of Technical Education, Faculty of Education, University Hradec Králové, Rokitanského 62,500 03 Hradec Králové, Czech Republic
cyrus@uhk.cz

ABSTRACT. This paper is dedicated to fatigue estimation of implants for spinal surgery. This article deals especially with special case of hollow pedicle screw. Implant systems utilizing specially designed spinal instrumentation are often used in these surgical procedures. The most common surgical procedure is spinal fusion, also known as spondylodesis, is a surgical technique used to join two or more vertebra. Implants are subjected to many loading cycles during their life, especially in the case of other degenerative changes in the skeleton, there are often changes in loading conditions, which often cannot be accurately determined. These changes often lead to further bending load in the thread. Hollow screws studied in this work show higher fatigue resistance than other types of implants.

KEYWORDS. Pedicle-screw; Titan alloy; Fatigue life; Finite element analysis.

INTRODUCTION

Pedicle screws are used for treating several types of spinal injuries. Together with rods and plates, they are used to form intrapedicular fixation or transpedicle screw devices [1-4] for spinal fusion. Fusing of the spine is used to eliminate the pain caused by abnormal motion of the vertebrae by immobilizing the faulty vertebrae or to treat most spinal deformities, such as scoliosis. Basicaly, this method involves the insertion However, screw breakage and loosening have been reported, which may create post-surgery problems [2]. Currently various types of pedicle screw are used: cylindrical and conical, hollow and solid. In this work are considered solid and hollow cylindrical screws.
Hollow screws are used for filling the wound with cement. Since the bone during drilling fulfills blood and other impurities, which could be the cause internal inflammation. Filling takes place through of a hollow screw. For filing are used various cements. In this work was used polymethyl methacrylate bone cement with multi-waled carbon nanotubes [5]. The prediction of fatigue failure is important forprevention of serious medical complications. For the fatigue life

prediction of pedicle-screws was used the method proposed by Navarro [6, 7, 8] and comparison with other methods used in multiaxial fatigue [9]. In the work, fatigue resistance of hollow pedicle-screw and solid pedicle-screws were compared.

MATERIALS CHARACTERIZATION

Screws used in this study were made of commercially titanium alloy 6AL4V ELI also known as Grade 23. It is an α-β phase titanium alloy made of 6% Al and 4% V in weight with a reduced content of interstitial elements such as oxygen and carbon (Extra Low Intersticials) and also iron. Chemical composition of material is shown in Tab. 1. This table compared the maximum value of the chemical elements specified by the manufacturer and the values measured by X-ray Spectrometers.

	C[%]	N[%]	O[%]	H[%]	V[%]	Al[%]	Fe[%]
Manufacturer	0.08	0.03	0.013	0.0125	3.5-4.5	5.5-6.5	0.25
Measurement	0.073	0.025	0.012	0.0113	4.12	6.015	0.17

Table 1: Chemical composition of titanium alloy Grade 23. In the first row are the maximal values of the elements specified by the manufacturer. In the second row line element values are obtained by measuring.

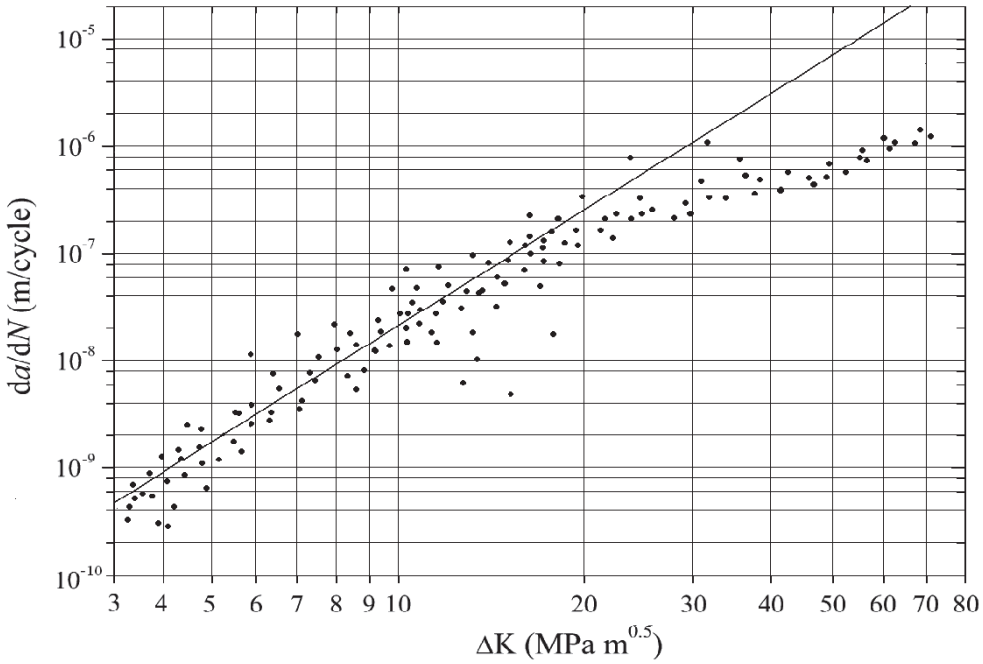

Figure 1: Crack growth rate of Grade 23 titanium alloy. The crack growth properties were measured on standard test method for measurement of fatigue crack growth rates introduced by ASTME 647.

Mechanical properties of material are: the Young modulus of this material is E = 104.5 GPa. Test were performed to determine the ultimate tensile strength, σ_u = 860 MPa and yield stress σ_y = 820 MPa. Further mechanical properties are elongation at break A = 14%, reduction area S_i = 25% and Vickers hardness 350 HV.
The crack growth properties were measured on Standard test method for measurement of fatigue crack growth rates introduced by ASTME 647 [9]. This test method covers the determination of fatigue crack growth rates from near-threshold to K_{max} controlled instability. Results are expressed in terms of the crack-tip stress-intensity factor range (ΔK), defined by the theory of linear elasticity. The experimental measurement was performed on specimen with diameter D_S = 4 mm. The measured properties, obtained constants are C = 5.1 10^{-12} and n = 4.2 for the crack growth in m/cycle, stress intesity factor K in MPa.m$^{0.5}$. The mechanical properties and biocompability of implant can be improved by surface

treatment. In this work, specimens with two types of surface treatment and implants without surface treatment were used. The first surface treatment was based on deposition TiO_2. The second deposition was based on TiN surface.
The both screws with surface treatment have a higher surface roughness than a screw without surface treatment. Roughness of a screw without treatment is R_a = 0.1 μm while roughnesses of the nitrided and TiO_2 covered screws are R_a = 2.7 μm and R_a = 3.1 μm.
The rougher surface improves the reception of the material by bones. Fig. 1 show experimental determination of Paris law for titanium alloy Grade 23. Paris law can be written for this material as:

$$\frac{da}{dN} = 5.1\ 10^{-12} \Delta K^{4.2} \tag{1}$$

Also fatigue test were carried out, results of these experiments are shown in Fig. 2. This figure shows fatigue curve (stress to number of cycle) *σ-N*. Fatigue test were carried out by room temperature on cylindrical specimen with diameter 4 mm. Loading frequency of fatigue experiment was 50 Hz and the loading was full reserve $R = -1$. In Fig. 2 is clearly visible reduction of fatigue limit for both types of surface treatments.

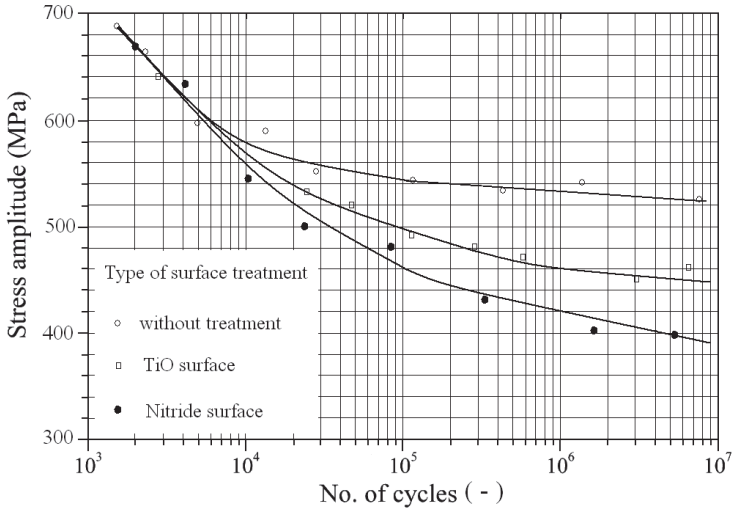

Figure 2: Fatigue curves in Grade 23 titanium alloy with surface layer TiO_2 and TiN and without surface treatment.

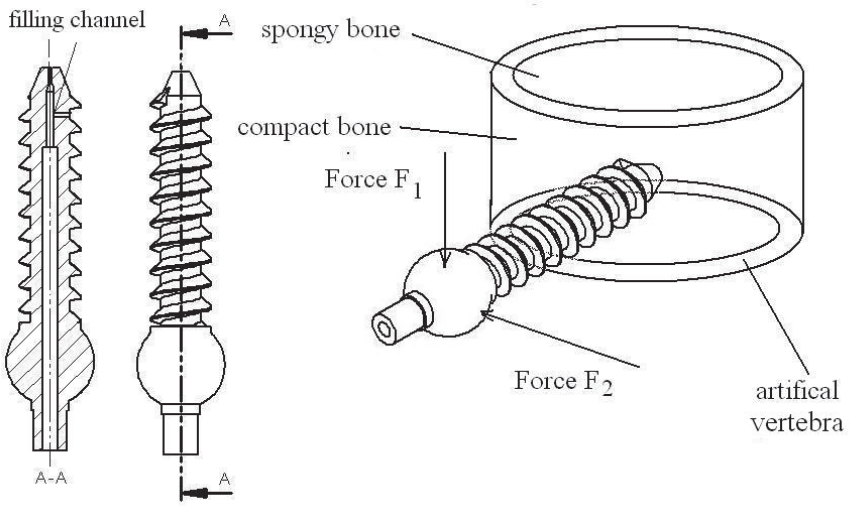

Figure 3: Specimen used in fatigue tests.

IMPLANT TESTING

For experiments wee used two types of pedicle-screw, the solid cylindrical and hollow screw. Both types have the same dimensions and geometry of thread. The implants were clamped in an artifical vertebra during test, so that the device simulates the bone-metal contact. The implants were subjected to bending loading. The pedicle-screw is loaded by a pair of forces perpendicular to the screw axis, the two forces are perpendicular to each other. Both forces are offset from the axis so that also create torque. The second bending force reaches its maximum when the first force reaches its second maximum, i. e. the period of the second load is doubled, i. e. $T_2 = 2T_1$. The experiments were carried to the final rapture of specimen. Final rapture is defiden as the complete fracture of the pedicle-screw.
Fracture appeared the point where the screw enters into the bone, I. e. at the point highest stresses. Since the bone consists of two basic parts, it is necessary to construct an artificial pedicle so that this fact was simulated. Surface of bone is composed from hard "compact bone" and cover layer of periosteum. The interior of the bone consists of a more flexible and softer tissue so-called "spongy bone". Artificial pedicle consists of two layers, a hard layer on the surface of 4 mm thick and the rest of the softer. The hollow bolt is fixed tightly by the entire length of the thread, whereas the vicinity of the thread is filled with cement everywhere. Schematic representation of the sample with loading forces is pictured in Fig. 3. During experiments the samples were loaded by this forces L_1 = 200, 300, 400, 500 N and L_2 = 50 N. The experiments were performed the room temperature and loading frequency was f_1 = 24 Hz respectively f_2 = 12 Hz.

NUMERICAL MODEL

3D-model of implant was prepared in SOLIDWORKS software and exported in ANSYS software. The model was meshed and solwed in ANSYS, see Fig.4. The aim of this model was determination of stress and strains in the pedicle-screw. Another finite element model was prepared for calculation of stress-intensity factor along the crack-path.

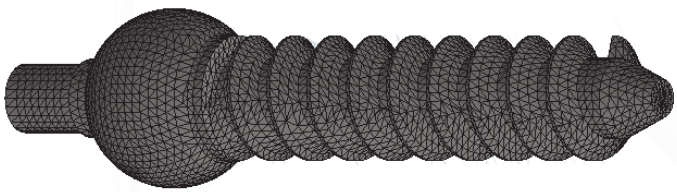

Figure 4: Meshed finite element model of pedicle screw.

First model of pedicle-screw is composed of 556.024 tetrahedral elements (type of element SOLID187) for solid, and 442.052 for hollow screw. In the case of solid screw, as model of the contacts between thread and bone for first 4 mm from point of entry into the bone was used null displacement, for the rest of the contact is allowed to move in a plane perpendicular to the axis of the screw (0.5 mm allowable displacement). Depth of hard part of bone corresponds to almost one loop of the thread. In the case of hollow screw. Conditions of null displacement were applied to all degrees of freedom (due the cement presence) of the nodes along the entire length of the thread in the bone.
For second model, model of the crack initiation area, is used refinement of net and the size of the elements is 5 μm, see Fig. 5. The important fact is, that in the region of crack initiation is elastoplastic deformation, while rest of volume is under elastic deformation. Plasticity of material was simulated kinematic hardening.

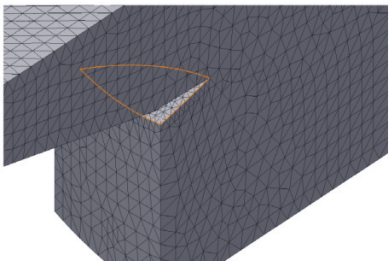

Figure 5: Meshed finite element model of crack.

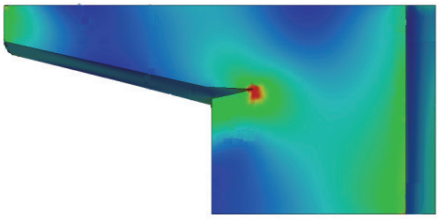

Figure 6: Von Misses stress in the thread.

Distribution of the von Mises stress obtained for elastic deformation of thread area of screw is shown in Fig.6. In this figure is clearly visible local maximum of stress concentration at the bottom of thread (lower diameter of thread). The crack initiates in this region. The evolution of normal stress along the crack path is displayed in Fig. 7, for four different loads.

For analysis of crack propagation phase is necessarily calculate the stress intensity factor at the bottom of thread, respectively at the forehead of crack. For this calculation second finite element model was prepared. For this model semieliptical crack is assumed. It is assumed, that the crack initiates on te lower diameter of thread and subsequently grows along the bottom of the thread (crack grows along the helix, with inclination 14.5°, which corresponds to the thread pitch) and propagates into core of the screw, see Fig. 8. The crack is characterized by two axes *a* and *b*, these two axis define the ellipse. The major axis is tangential to the thread and the secondary axis is perpendicular to the axis of the helix, respectively to the axis of screw.

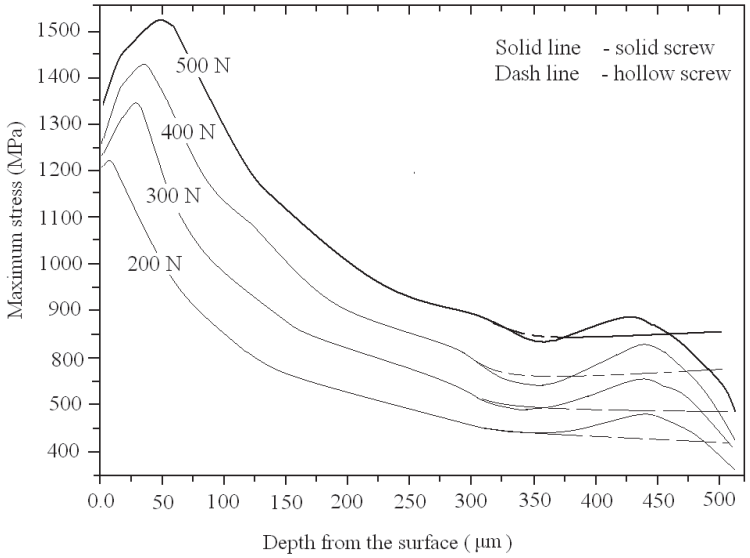

Figure 7: The evolution of normal stress along the crack path, for four different loads (200 N, 300 N, 400 N, 500 N).

When the diameter of crack is smaller then 50 μm, it is assumed that the crack flat. This assumption cannot be used for crack diameter greater then 50 μm. For greater crack is necessarily use submodelling, becose the number of elements is too large. The calculation of stress-intensity factor at the front of crack was based on *J*-integral method. For calculation was assumed that the material can be characterized by linear elastic deformation.

Stress-intensity factor is a function of crack length *a*. This relations is can be determined by repeated simulations. The lenght of crack at the start of simulation was 5 μm. This length is much smaller than the initial crack length for the propagation phase. With Paris' Law, a relationship

$$\Delta a_S = \Delta a_D \left(\frac{\Delta K_S}{\Delta K_D} \right)^n \tag{2}$$

can be obtained where Δa_S and Δa_D are increments of crack on surface and deepest poit of crack. The ΔK_S and ΔK_D are appropriate increments of stress-intensity factors and n is exponent in Paris law. With new increment of Δa_S, crack length at the surface changed and a new finite element model can be solved and the stress-intensity factor calculated. This process is repeated by software until the final length of crack is reached.

The shape changes in the process of crack growth can be described by the ratio a/b, where a and b are values corresponding to the lengths axis of the ellipse. Relations between ratio a/b and the length of crack is shown in Fig. 9. A sharp decline in the ratio a/b (see Fig. 9) indicates that the crack propagates faster along the helix (around the circumference of the screw cylinder) then into body of material. The following figure shows realitions between crack intensity factor (at the bottom of the thread) and crack length. Gradient of stress-intensity factor is is much greater at the

beginning of process, see Fig. 10. The stress intensity factor grows much faster at the surface of screw. Therefore, it is necessary to implement a plurality of simulations for the initial phase of the process.

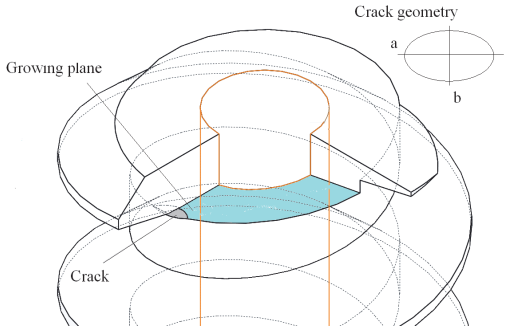

Figure 8: Crack in the thread, growing plane.

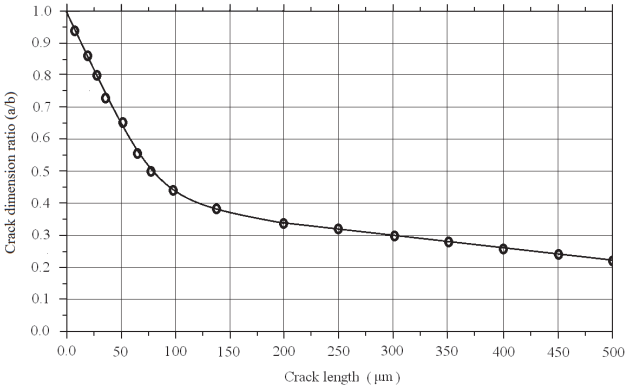

Figure 9: Relations between ratio a/b and the length of crack.

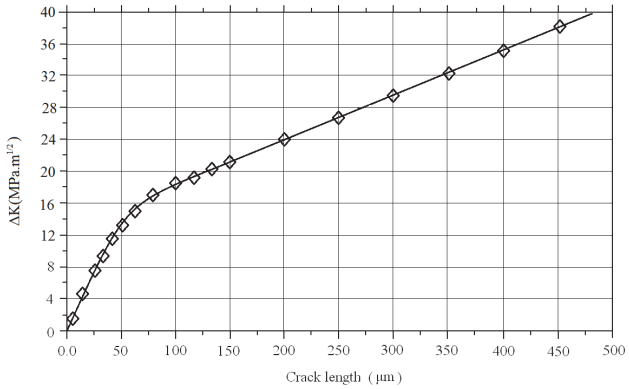

Figure 10: Relations between gradient of stress-intensity factor and the length of crack.

THEORETICAL MODEL

For theoretical analysis of fatigue process was used new method proposed by Navarro [7, 8] and multiaxial fatigue criteria modified for notched specimens were tested [9]. Model proposed by Navarro combined initiation and propagation phase, without the need to define boundary length of crack, to differentiate between the two phases of crack growth. It is necessary, To calculate the number of cycles needed to reach the length a (curve a-N_i, is necessary to know fatigue curve σ-N. The fatigue curve σ-N is in Fig. 1. This curve can be expressed by parameters obtained from

some multiaxial fatigue criteria, becose the pedicle screw is under multiaxial loading. If Fatemi-Socie criteria is used, so-called "initiation curves" can obtained [6, 7, 8], see Fig. 11.
In the Fig. 11 initiations curves for length of crack a_1 and a_2 are displayed. These curves shows the number of cycles required to achieve a crack length a_1, respectively a_2 , if Fatemi-Socie parameters FS are known. The damage parameter is given by the equation:

$$FS = \frac{\Delta\gamma_{\max}}{2}\left(1 + k\frac{\sigma_{\max}}{\sigma_y}\right) \tag{3}$$

In this equation, $\Delta\gamma_{max}$ is the shear strain increment in the plane where it has maximum value, k is a constant that is obtained from the fatigue tests, σ_{max} is the normal stress perpendicular to the plane where is the maximum shear strain, and σ_y is the yield strength. The number of cycle can be calculated by equation

$$N_i\left(FS, a\right) = N_{Total}\left(FS\right) - \int_a^{a^f} \frac{da}{C\Delta K^n} \tag{4}$$

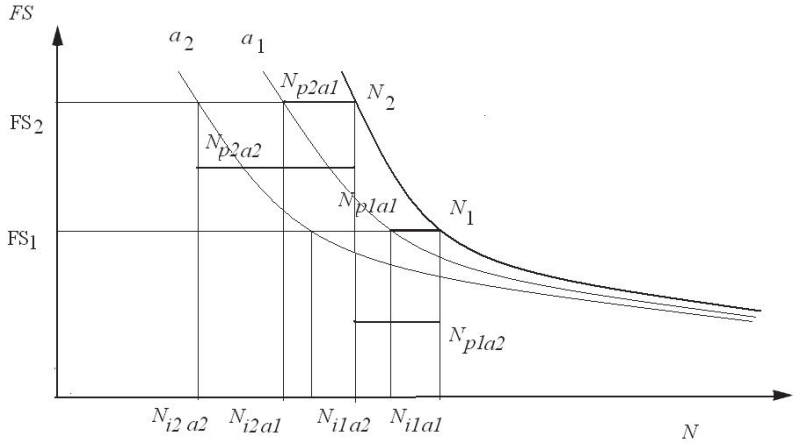

Figure 11. Initiations curves for length of crack a_1 and a_2

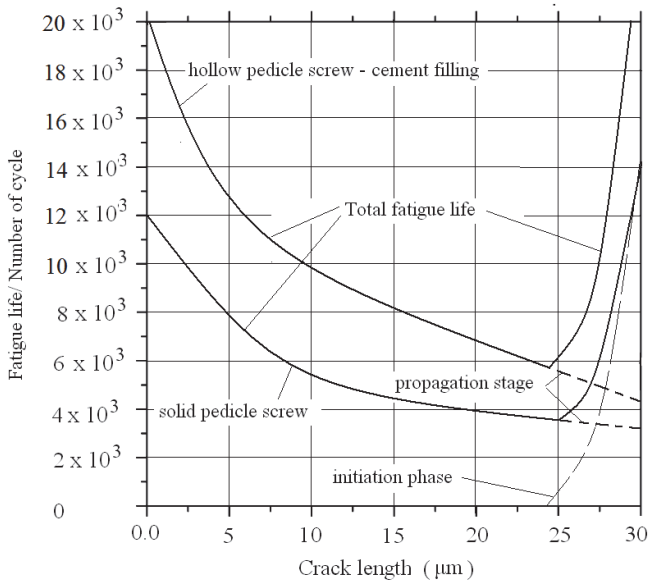

Figure 12. Application of the prediction model in the test with F = 400 N (Nitrided pedicle screw).

In propagation stage, the number of cycles needed to propagate a crack to final failure, is calculated using fracture mechanics. This phase is described by the curve a-N_P. This curve is obtained by integration of growth law for any crack length to failure. The growth law can be expressed as

$$\frac{da}{dN} = C\left(\Delta K^n - \left(\Delta K_{th,Long}\left(\frac{a^f}{a^f - a_0^f - l_0^f}\right)^{\frac{1}{2}f}\right)^n\right) \tag{5}$$

where $\Delta K_{th,Long}$ is the growth threshold for long cracks, f is a parameter (for this case f = 2.5), a_0 is the El Haddad parameter [11, 12] and l_0 is the average distance to the first microstructural barrier. El Haddad parameter is defined as

$$a_0 = \frac{1}{\pi}\left(\frac{K_{th,Long}}{\Delta\sigma_{FL}}\right)^2 \tag{6}$$

where $\Delta\sigma_{FL}$ is the fatigue limit of the material. The growth of threshold for long cracks in Eq. 5 was multiplicated by factor which was derived from the theoretical approximation of the Kitagawa–Takahashi diagram [13,14]. The stress intensity factor is can be calculated as

$$K_I(a) = \sqrt{\frac{2}{\pi}}\int_0^2 \frac{1}{\sqrt{S}}\left(1 + m_1\frac{S}{a} + m_2\left(\frac{S}{a}\right)^2\right)\sigma(S)\,dS \tag{7}$$

where σ is the stress normal to the growth plane of the crack and S is a coordinate running through the crack from the tip of crack to the surface. S and a parameters depend on the dimensions of the cross section of the specimen and crack length. When two curves (number of cycles to length and number of cycles to rupture, a-N_i and a-N_p) are known, they can be merged, so that the entire fatigue life can be described. This curve for total life of screw is shown in Fig. 12. From this picture is clearly visible, that the initiation life is much smaller than propagation life.

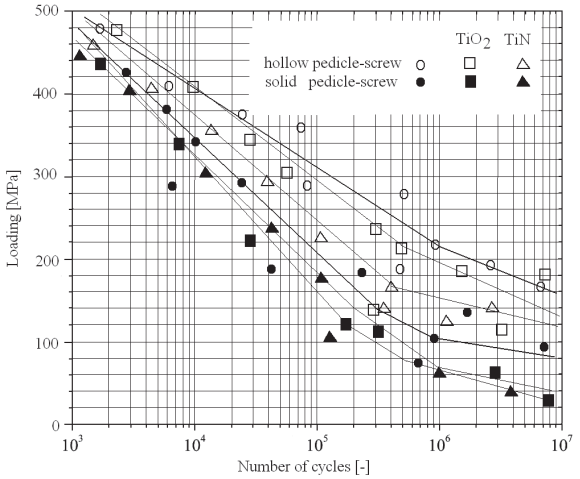

Figure 13: Fatigue tests in implants and theoretical prediction.of hollow and solid pedicle screws. Symbols: specimen without treatement – circle, nitride surface – square, oxide surface triangle.

RESULTS

Hollow screws show higher fatigue resistance at the same load than full screws. This could be explained with more suitable distribution of stress along thread. Results of experimental load of pedicle-screw are shown at Fig. 13. Fig. 13 shows that the crack initiation phase is about 10 % of fatigue life of implant.

This figure shows also curves of theoretical lifespan obtained with help of a model based on Navarro method. Other methods of lifespan forecast have been tested for a comparison with our new method. In article [9], there are described various multiaxial criteria, adapted for lifespan forecast of notched samples, which corresponds to the case of the screw. A criterion proposed by Goncalves gives the best forecast of all criteria described in [9]. Goncalves criterion has been modified with help of A_G and B_G parameters for sample analysis.

$$A_G \cdot a_{GAM} \sqrt{\sum_{i-1}^{5} d_i^2} + B_G \cdot b_{GAM} \cdot \sigma_{1.\max} \le f_{-1} \tag{8}$$

and

$$d_i = \left(\max\left(s_i(t)\right) - \min\left(s_i(t)\right)\right)/2\,, \tag{9}$$

where parameters d_i can be determined from minimum and maximum values of the transformed deviatoric stress tensor. The material variables are set from fatigue limits as:

$$a_G = \frac{\kappa - 1}{\sqrt{2}\left(1 - 1/\sqrt{3}\right)}, \tag{10}$$

$$b_G = \frac{\sqrt{3} - \kappa}{\sqrt{3} - 1}. \tag{11}$$

If we perform a comparison of theoretical lifespan forecast of the screw based on Navarro method [6, 7, 8], and older methods [9] (Goncalves method is best of them), it can be said that Navarro method gives 50 % better result than Goncalves method. Navarro method respects conditions of fixation of the screw in the bone better than older methods. The most important advantage of Navarro method is a possibility of including an influence of filling cement.

CONCLUSIONS

Hollow screws with the performance show higher fatigue resistance with the same load, which can be explained by stronger deposition over the entire length of the screw. Results of fatigue test were compared with theoretical predictions and theoretical model predicts that initiation phase is about 10% of fatigue life of implant.

REFERENCES

[1] Chen, C.S., Chen, W.J., Cheng, C.K., Jao, S.H., Chuech, S.C., Wang, S.C., Failure analysis of broken pedicle screws on spinal instrumentation, Medical Engineering & Physics, 27 (2005) 487–496. DOI:10.1016/j.medengphy.2004.12.007.

[2] Griza, S., de Andrade, C.E.C., Batista, W.W, Tentardini, E.K., Strohaecker, T.R., Case study of Ti6Al4V pedicle screw failures due to geometricand microstructural aspects, Engineering Failure Analysis, 25 (2012) 133–143. DOI:10.1016/j.engfailanal.2012.05.009.

[3] Amaritsakul, Y., Ching-Kong , Ch., Jinn, J., Biomechanical evaluation of bending strength of spinal pedicle screws, including cylindrical, conical, dual core and double dual core designs using numerical simulations and mechanical tests, Medical Engineering & Physics, 36 (2014) 1218–1223. DOI: 10.1016/j.medengphy.2014.06.014.

[4] Krag, M. H., Biomechanics of thoracolumbar spinal fixation: a review, Spine, 16 (1991) 84–99.

[5] Ormsby, R. McNally, T., Oharre, P., Burke, G., Mitchell, G., Fatigue and biocompability of properties of poly(methyl methacrylate) bone cement with multi-waled carbon nanotubes, Acta Biamaterialia 8 (2012) 1201–1212. DOI: 10.1016/j.actbio.2011.10.010.

[6] Ayllón, J.M, Navarro, C., Vázquez, J., Domínguez, J., Fatigue life estimation in dental implants, Engineering Fracture Mechanics, 123 (2014) 34–43. DOI:10.1016/j.engfracmech.2014.03.011.

[7] Navarro, C., Muńoz, S., Domínguez, J., On the use of multiaxial fatigue criteria for fretting fatigue life assessment, Int J Fatigue, (2008) 32–44. DOI:10.1016/j.ijfatigue.2007.02.018.
[8] Navarro, C., Vázquez, J., Domínguez, J., A general model to estimate life in notches and fretting fatigue. Engineering Fracture Mechanics, (2011) 1590–601. DOI:10.1016/j.engfracmech.2011.01.011.
[9] Major, S, Hubálovský, S., Kocour, V., Valach, J., Effectiveness of the Modified Fatigue Criteria for Biaxial Loading of Notched Specimen in High-Cycle Region, Applied Mechanics and Materials, 732 (2015) 63-70. DOI: 10.4028/www.scientific.net/AMM.732.63.
[10] ASTM E647. Standard test method for measurement of fatigue crack growth rates. West Conshohocken, PA, United States, http://www.astm.org/Standards/E647.htm.
[11] Lazzarin, P., Tovo, R., Meneghetti, G,. Fatigue crack initiation and propagation phases near notches in metals with low notch sensitivity. Int J Fatigue, 19 (1997) 647–65. DOI:10.1016/S0142-1123(97)00091-1.
[12] El Haddad, M.H., Topper, T.H., Smith, K.N., Prediction of non-propagating cracks, Engineering Fracture Mechanics, 11 (1979) 573–584. DOI: 10.1016/0013-7944(79)90081-X.
[13] Kitagawa, H., Takahashi, S., Applicability of fracture mechanics to very small cracks or the cracks in the early stage, In: Proceedings of the Second International Conference on Mechanical Behavior of Materials. Metals Park, OH: ASM; (1976) 627–31.
[14] Peters, J.O., Boyce, B.L., Chen, X., McNaney, J.M., Hutchinson, J.W., Ritchie, R.O., On the application of the Kitagawa–Takahashi diagram to foreign-object damage and high-cycle fatigue, Engineering Fracture Mechanics. 69 (2002) 1425–1446. DOI:10.1016/S0013-7944(01)00152-7.